

Separation of ion components produced by plasma-assisted catalytic ionization

W. Oohara, T. Hibino, T. Higuchi, and T. Ohta

Citation: *Rev. Sci. Instrum.* **83**, 083509 (2012); doi: 10.1063/1.4748273

View online: <http://dx.doi.org/10.1063/1.4748273>

View Table of Contents: <http://rsi.aip.org/resource/1/RSINAK/v83/i8>

Published by the [American Institute of Physics](http://www.aip.org).

Related Articles

Ionization enhancement in silicon clusters and germanium atoms in the presence of zirconium

J. Chem. Phys. **137**, 194312 (2012)

Formation of negative hydrogen ion: Polarization electron capture and nonthermal shielding

J. Chem. Phys. **137**, 094310 (2012)

Ionization energy of atoms obtained from GW self-energy or from random phase approximation total energies

J. Chem. Phys. **136**, 194107 (2012)

Scattering of nitrogen molecules by silver atoms

J. Chem. Phys. **136**, 164305 (2012)

Rotational excitation of H₂O by para-H₂ from an adiabatically reduced dimensional potential

J. Chem. Phys. **136**, 094109 (2012)

Additional information on Rev. Sci. Instrum.

Journal Homepage: <http://rsi.aip.org>

Journal Information: http://rsi.aip.org/about/about_the_journal

Top downloads: http://rsi.aip.org/features/most_downloaded

Information for Authors: <http://rsi.aip.org/authors>

ADVERTISEMENT



AIP Advances

Now Indexed in Thomson Reuters Databases

Explore AIP's open access journal:

- Rapid publication
- Article-level metrics
- Post-publication rating and commenting

Separation of ion components produced by plasma-assisted catalytic ionization

W. Oohara, T. Hibino, T. Higuchi, and T. Ohta

Department of Electronic Device Engineering, Yamaguchi University, Ube 755-8611, Japan

(Received 22 May 2012; accepted 12 August 2012; published online 31 August 2012)

Positive and negative hydrogen ions are produced by plasma-assisted catalytic ionization using a porous nickel plate, where the irradiation current density and energy of positive ions produced by discharge to the porous plate are controlled. The ion energy distributions are analyzed from the properties of current densities of positive and negative ions extracted from the porous surface. Positive ions passing through fine pores of the porous plate and positive and negative ions produced on the porous surface are observed. It is clarified that the produced fluxes of positive and negative ions and the flux balance between them are controlled by the irradiation current density and energy, respectively.

© 2012 American Institute of Physics. [<http://dx.doi.org/10.1063/1.4748273>]

I. INTRODUCTION

The research and development of negative-ion sources^{1,2} has been extensively performed in connection with neutral beam injection heating for fusion-oriented plasmas^{3,4} and ion guns for proton accelerators.^{5,6} A small admixture of cesium vapor in a hydrogen discharge significantly improves negative-ion production and decreases the current of coextracted electrons.^{7,8} However, the use of cesium complicates the ion-source operation and requires the careful stabilization of cesium injection and discharge parameters. The production of negative ions without using cesium is desirable from the viewpoint of the ion-source operation. There have been many attempts to develop negative-ion sources with an acceptable negative-ion beam emittance but without a cesium admixture. In volume production, a highly vibrationally excited hydrogen molecule effectively captures a low-energy plasma electron to form a negative ion through dissociative electron attachment.⁹⁻¹³ However, there is a relatively low current density of negative ions in volume production.

We are interested in not only ion production, but also plasma physics. A typical plasma consists of electrons and positive ions, and the asymmetric diversity of collective plasma phenomena is caused by their large mass difference. In contrast, a pair plasma consists of only positively and negatively charged particles of equal mass. Pair plasmas, for example, those consisting of positrons and electrons, maintain space-time symmetry because their particle mobilities in electromagnetic fields are the same. Pair plasmas represent a new state of matter with unique thermodynamic properties markedly different from those of conventional plasmas.¹⁴⁻¹⁹ However, it is not easy to generate and maintain an electron-positron plasma; therefore, we have focused on the steady-state generation of a pair-ion plasma consisting of positive and negative ions with an equal mass.²⁰⁻²² Hydrogen atomic pair ions, i.e., H^+ and H^- ions, are the lightest ions and have high response frequencies to electromagnetic fields. To generate a hydrogen pair-ion plasma, the production of equal quantities of H^+ and H^- ions and the absence of impurities, such as electrons and other ions, are required. It is difficult to satisfy these

requirements in surface production with a cesium admixture or in volume production. To overcome this difficulty, we have proposed a plasma-assisted catalytic ionization method for the production of positive and negative hydrogen ions.²³⁻²⁶ When positive hydrogen ions produced by discharge are irradiated to a porous catalyst, the hydrogen ions are produced from the back of the irradiation plane. In this paper, the properties of the produced ions are discussed in detail.

II. EXPERIMENT

A hydrogen plasma is generated by a dc arc discharge between filament cathodes and a wall anode in a cuboidal chamber with a cross section of 25 cm \times 25 cm, i.e., a bucket plasma source. The cathodes are four horseshoe tungsten filaments of 0.7 mm diameter and 15 cm length, which are biased at a discharge voltage of $V_d = -70$ V, at which the plasma density is maximized to about 3×10^{11} cm⁻³ at a discharge power of $P_d = 700$ W. The plasma generated in the field-free region is surrounded by line-cusp magnetic fields near the grounded chamber wall. The diffusion of the plasma to the wall is thus reduced, resulting in the highly efficient generation of a uniform plasma. Figure 1 shows a schematic diagram of the experimental setup. A commercially available Ni porous plate (CELMET, Sumitomo Electric Toyama Co., Ltd.) with a pore size of 0.45 mm, a thickness of 1.4 mm, a specific surface area of 5800 m²/m³, and a porosity of 96.6% is used as a catalyst. The porous plate is negatively biased at a dc voltage of V_{pc} and then irradiated with positive ions. Since the circular irradiation area is 6.1 cm² (diameter of 2.8 cm) and the other electrode is covered with a mica limiter plate, the irradiation current density J_{ir} applied to the porous plate can be obtained. The porous plate is located at $z = 0$ cm, and the discharge section corresponds to the region $z < 0$ cm. Plasma parameters in the region are measured using a Langmuir probe at $z = -7$ cm. The back of the irradiation plane is covered with an SUS304 limiter plate with a circular aperture of area 1.3 cm² (diameter of 1.3 cm). Positive ions are accelerated up to $e(\phi_s - V_{pc})$ (eV) in the sheath formed in front of

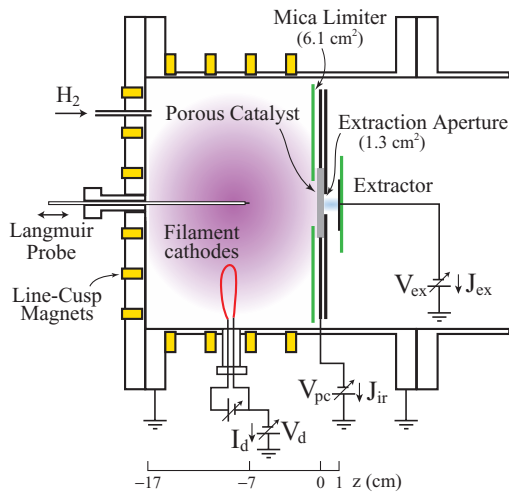


FIG. 1. Diagram of experimental setup. The hydrogen plasma generated in the bucket source is irradiated to the Ni porous catalyst. The extraction current of ions, which are produced from the back of the irradiation plane by plasma-assisted catalytic ionization, is analyzed.

the porous plate, where the plasma potential ϕ_s at $z = -7$ cm is at around +10 V when $V_{pc} < 0$ V and $P_d > 100$ W. The irradiation energy is controlled by adjusting V_{pc} . The irradiation energy is proportional to V_{pc} , because the plasma potential fluctuation is very small compared with V_{pc} .²⁶ The hydrogen pressure in the source during operation is about 0.1 Pa.

Positive and negative ions are produced and an ionic plasma is generated in the region $z > 0$ cm. When the ion extractor shown in Fig. 1 is removed, a Langmuir probe is set at $z = 3$ cm (not shown here). Positive- and negative-saturation currents, I_+ and I_- , are obtained at probe bias voltages of -120 V and $+120$ V, respectively. The dependencies of I_+ and I_- on the irradiation energy $e(\phi_s - V_{pc})$ are shown in Fig. 2. I_- monotonically increases with the irradiation energy. I_+ also tends to increase with the irradiation energy, but there are two broad peaks at different irradiation energies at a given J_{ir} . Furthermore, both I_+ and I_- increase proportionally with the irradiation current density. The irradiation current density can be varied by adjusting the discharge power because the plasma density in the region $z < 0$ cm depends on the power. The peak energies increase with the irradiation current density.²⁵ The probe current is collected from the ionic plasma, not directly from the porous-catalyst surface.

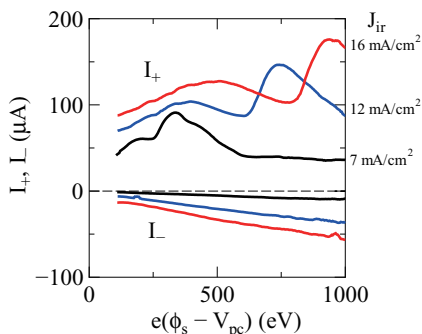


FIG. 2. Probe saturation currents of positive and negative ions as a function of irradiation energy.

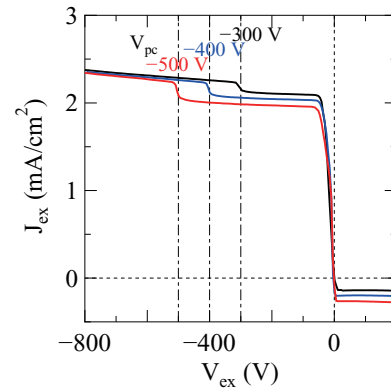


FIG. 3. Extraction current density J_{ex} –voltage V_{ex} characteristics obtained from extractor.

The ionic plasma potential is close to ϕ_s . Negative ions are accelerated in the sheath formed in front of the catalyst and become fast because of $\phi_s > V_{pc}$. On the other hand, positive ions are decelerated in the sheath and become slow. A part of positive ions is reflected in the sheath, the positive-ion flux is self-regulated to sustain quasi-neutrality. Thus, the probe saturation currents do not necessarily indicate the quantity of ions produced.

Currents of positive and negative ions extracted from the back of the irradiation plane are measured using the ion extractor in Fig. 1. The extractor is located at a distance of 1 cm from the porous plate. The ions, free from the influence of the sheath, are extracted by an electric field applied between the porous plate and the biased electrode and then collected all the ions by the electrode. Since the extraction aperture area is 1.3 cm², the extraction current density J_{ex} can be obtained. Typical extraction current density (J_{ex})–voltage (V_{ex}) characteristics are shown in Fig. 3. The positive current is much higher than the negative current, in common with the relation between I_+ and I_- .

The $J_{ex} - V_{ex}$ characteristics have two inflection points. One is at $V_{ex} \sim V_{pc}$ and the other is at $V_{ex} \sim 0$ V. The kinetic-energy distributions are calculated by differentiating the $J_{ex} - V_{ex}$ characteristics, where the reference potential in the region $z > 0$ cm is the porous-plate potential (V_{pc}) because all the ions are emitted from the porous surface. The energy distributions in the cases of a constant irradiation current ($J_{ir} = 15$ mA/cm²) and a constant irradiation energy ($e(\phi_s - V_{pc}) = 610$ eV) are shown in Figs. 4(a) and 4(b), respectively. There are two components of the ions in the energy distributions determined by taking the reference potential into consideration. The kinetic energy of the high-energy component increases with the irradiation energy as shown in Fig. 4(a). Thus, the high-energy component at $e(V_{ex} - V_{pc}) \sim e(\phi_s - V_{pc})$ consists of passing positive ions that are part of the irradiated positive ions passing through the porous plate that reacted with the porous surface, because the energy is slightly lower than the irradiation energy. The quantity of passing positive ions is independent of the irradiation energy, but depends on the irradiation current density. The kinetic energy of the low-energy component is independent of the irradiation energy. The low-energy component at $e(V_{ex} - V_{pc})$

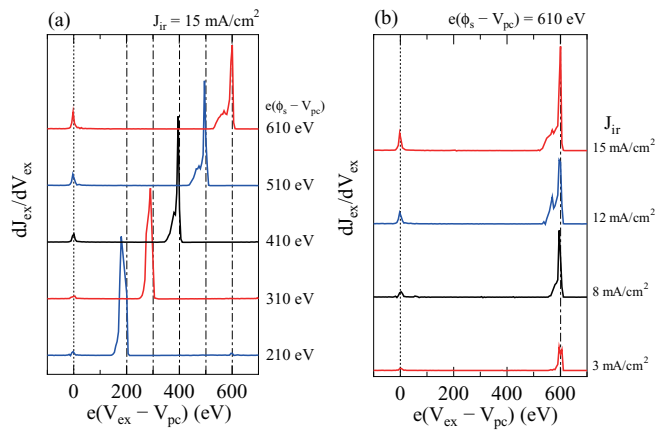


FIG. 4. Dependence of ion energy distribution calculated from $J_{ex} - V_{ex}$ characteristics on irradiation energy (a) and irradiation current density (b), where the reference potential is the catalyst voltage V_{pc} .

$\sim 0 \text{ eV}$ consists of positive ions produced by desorption ionization with a kinetic energy less than 10 eV. The quantity of the low-energy component increases proportionally with the irradiation current density as shown in Fig. 4(b). The negative current can be detected at $e(V_{ex} - V_{pc}) > e(\phi_s - V_{pc})$ because positive ions cannot be detected. Negative ions will start to be produced at $V_{ex} \sim V_{pc}$ or $V_{ex} \sim \phi_s$, where their energy will be low. It is not clear at present which potential they start to be produced. The potential is concerned with the production mechanism of negative ions. There is a possibility that the negative current consists of negative ions and electrons in the case of using the porous catalyst. (1) Positive ions passing through the fine pores of porous catalyst strike on adsorbed hydrogen atoms, and negative ions are produced by desorption ionization. (2) Positive ions are transmitted through bulk metal, and negative ions are produced from positive ions detached from the surface. (3) Electrons are produced by secondary emission due to fast ion impact. The probe saturation currents of I_+ and I_- are $I_+ > I_-$ in the ionic plasma. If the electron density is not vanishingly low, I_- will be higher than I_+ . Thus, we think that the electron flux will be vanishingly low and negative ions will be mainly produced by desorption ionization at $V_{ex} \sim V_{pc}$ in the case of (1).

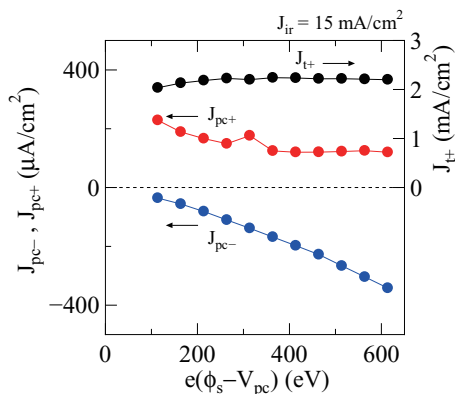


FIG. 5. Dependence of current density of passing positive ions and current densities of positive and negative ions produced on the catalyst at $J_{ir} = 15 \text{ mA/cm}^2$ on irradiation energy.

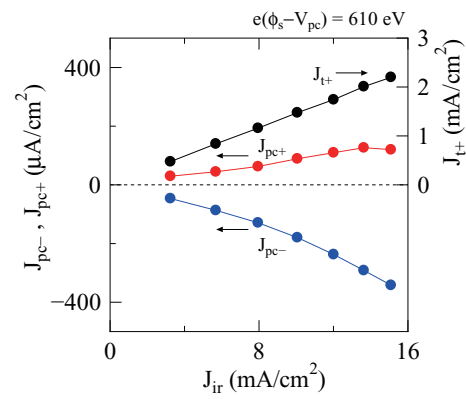


FIG. 6. Dependence of current density of passing positive ions and current densities of positive and negative ions produced on the catalyst at $e(\phi_s - V_{pc}) = 610 \text{ eV}$ on irradiation current density.

The current densities of the produced positive and negative ions, J_{pc+} and J_{pc-} , and the current density of passing positive ions, J_{t+} , can be separately measured by utilizing their energy difference. The dependencies of J_{pc+} , J_{pc-} , and J_{t+} on the irradiation energy and the irradiation current density are shown in Figs. 5 and 6, respectively. The passing positive ions are detected at $V_{ex} \leq V_{ps}$. The produced positive and negative ions are detected at $V_{ex} \leq V_{pc}$ and $V_{ex} \geq V_{pc}$, respectively. J_{t+} is defined as $J_{ex}(V_{ex} = -80 \text{ V}) - J_{ex}(V_{ex} = +10 \text{ V})$. J_{pc+} and J_{pc-} are defined as $J_{ex}(V_{ex} = -800 \text{ V}) - J_{t+}$ and $J_{ex}(V_{ex} = +100 \text{ V})$, respectively, where $J_{ex}(V_{ex} = +10 \text{ V}) \sim J_{ex}(V_{ex} = +100 \text{ V})$. The extraction current of positive ions at $V_{ex} < V_{pc}$ depends on V_{ex} and is almost independent of V_{pc} as shown in Fig. 3. To prevent the increase in extraction current caused by the electric field used for extraction, the extraction voltage is fixed at $V_{ex} = -800 \text{ V}$ or $+100 \text{ V}$ independent of V_{pc} . J_{pc-} increases both with the irradiation energy under a constant irradiation current density and with the irradiation current density under a constant irradiation energy. J_{t+} and J_{pc+} are approximately constant under a constant irradiation current density and increase with the irradiation current density. Thus, the quantities of positive and negative ions produced depend on the irradiation current density.

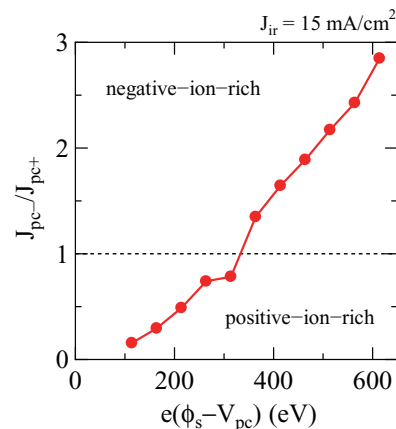


FIG. 7. Dependence of current density ratio at $J_{ir} = 15 \text{ mA/cm}^2$ on irradiation energy.

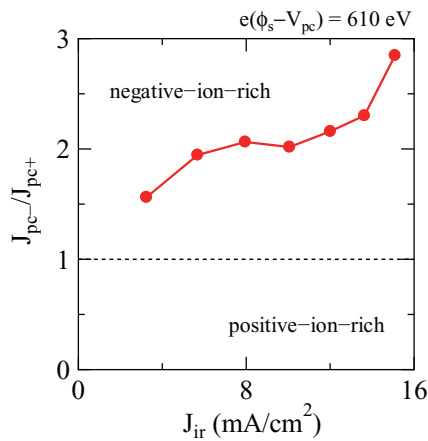


FIG. 8. Dependence of current density ratio at $e(\phi_s - V_{pc}) = 610$ eV on irradiation current density.

The dependence of the current density ratios J_{pc-}/J_{pc+} on the irradiation energy and the irradiation current density are shown in Figs. 7 and 8, respectively, where the sign of the current density is ignored because the ion flux is being compared. J_{pc-}/J_{pc+} increases with the irradiation energy according to Fig. 7, and the ion production property is changed by the irradiation energy from a positive-ion-rich state to a negative-ion-rich state. The state at $e(\phi_s - V_{pc}) = 610$ eV is negative-ion-rich and independent of J_{ir} ; however, the ratio is shifted with changes in J_{ir} . Therefore, the balance between the production of positive and negative ions, i.e., the production efficiency of negative ions, mainly depends on the irradiation energy.

III. SUMMARY

A plasma-assisted catalytic ionization method for the production of positive and negative hydrogen ions has been proposed for generating a hydrogen pair-ion plasma and developing a highly efficient hydrogen negative-ion source without a Cs admixture. The ionization method involves the following steps: positive ions in discharge plasmas are irradiated to a porous catalyst, and positive and negative ions are produced from the back of the irradiation plane. An ionic plasma is generated on the back surface. The ion fluxes produced are estimated by measuring the Langmuir-probe saturation currents in the ionic plasma. However, the saturation currents are not necessarily proportional to the ion fluxes emitted from the porous catalyst, because the ion fluxes are affected by the sheath formed in front of the porous catalyst. The properties

of the extraction current densities of positive and negative ions from the catalyst surface are measured when an electric field is directly applied to the catalyst surface. The presence of positive ions passing through the porous catalyst and positive and negative ions produced on the catalyst surface is observed in the ion-energy distributions obtained from the properties. The extraction current densities of the positive and negative ions can be separately obtained by utilizing their energy difference. It was found that the produced fluxes of positive and negative ions and the flux balance between them are mainly controlled by the irradiation current density and the irradiation energy, respectively.

ACKNOWLEDGMENTS

The authors thank Dr. K. Tsumori and Dr. Y. Takeiri for their collaboration and Dr. O. Fukumasa for his encouragement. This work was partially supported by a grant-in-aid for Scientific Research (C) of JSPS (23540575) and the collaboration program of National Institute for Fusion Science (NIFS11KOAR013) in Japan.

- ¹R. Middleton and C. T. Adams, *Nucl. Instrum. Methods* **118**, 329 (1974).
- ²J. Ishikawa, "Negative ion sources," in *The Physics and Technology of Ion Sources*, 2nd ed., edited by I. G. Brown (Wiley VCH, Weinheim, 2004), p. 285.
- ³L. R. Grisham, *IEEE Trans. Plasma Sci.* **36**, 1512 (2008).
- ⁴Y. Takeiri, *Rev. Sci. Instrum.* **81**, 02B114 (2010).
- ⁵H. Oguri, Y. Okumura, K. Hasegawa, Y. Namekawa, and T. Shimooka, *Rev. Sci. Instrum.* **73**, 1021 (2002).
- ⁶A. Ueno, K. Ikegami, and Y. Kondo, *Rev. Sci. Instrum.* **75**, 1714 (2004).
- ⁷K. N. Leung and K. W. Ehlers, *Rev. Sci. Instrum.* **53**, 803 (1980).
- ⁸G. D. Alton, *Surf. Sci.* **175**, 226 (1986).
- ⁹M. Bacal and G. W. Hamilton, *Phys. Rev. Lett.* **42**, 1538 (1979).
- ¹⁰M. Bacal and A. M. Bruneteau, *AIP Conf. Proc.* **111**, 31 (1984).
- ¹¹K. N. Leung and K. W. Ehlers, *AIP Conf. Proc.* **111**, 67 (1984).
- ¹²Y. Okumura, M. Hanada, T. Inoue, H. Kojima, Y. Matsuda, Y. Ohara, M. Seki, and K. Watanabe, *AIP Conf. Proc.* **210**, 169 (1990).
- ¹³O. Fukumasa and S. Mori, *Nucl. Fusion* **46**, S287 (2006).
- ¹⁴G. A. Stewart and E. W. Laing, *J. Plasma Phys.* **47**, 295 (1992).
- ¹⁵N. Iwamoto, *Phys. Rev. E* **47**, 604 (1993).
- ¹⁶G. P. Zank and R. G. Greaves, *Phys. Rev. E* **51**, 6079 (1995).
- ¹⁷C. M. Surko, M. Leventhal, and A. Passner, *Phys. Rev. Lett.* **62**, 901 (1989).
- ¹⁸M. D. Tinkle, R. G. Greaves, and C. M. Surko, *Phys. Plasmas* **2**, 2880 (1995).
- ¹⁹E. P. Liang, S. C. Wilks, and M. Tabak, *Phys. Rev. Lett.* **81**, 4887 (1998).
- ²⁰W. Oohara and R. Hatakeyama, *Phys. Rev. Lett.* **91**, 205005 (2003).
- ²¹W. Oohara, D. Date, and R. Hatakeyama, *Phys. Rev. Lett.* **95**, 175003 (2005).
- ²²W. Oohara and R. Hatakeyama, *Phys. Plasmas* **14**, 055704 (2007).
- ²³W. Oohara and O. Fukumasa, *J. Plasma Fusion Res. SERIES* **8**, 860–864 (2009).
- ²⁴W. Oohara and O. Fukumasa, *Rev. Sci. Instrum.* **81**, 023507 (2010).
- ²⁵W. Oohara, T. Maeda, and T. Higuchi, *Rev. Sci. Instrum.* **82**, 093503 (2011).
- ²⁶W. Oohara, T. Maeda, and T. Higuchi, *AIP Conf. Proc.* **1390**, 430 (2011).